K-vacancy production by 4.88-GeV protons

R. Anholt,* S. Nagamiya, J. O. Rasmussen, H. Bowman, J. G. Ioannou-Yannou, and E. Rauscher
Lawrence Berkeley Laboratory, University of California, Berkeley, California 94720
(Received 13 November 1975; revised manuscript received 13 August 1976)

Cross sections for K-vacancy production by 4.88-GeV protons on elements between Ni and U have been measured. These cross sections lie approximately a factor of 1.4 to 2.5 above the plane-wave Born-approximation predictions. To partially explain these deviations, we argue that an additional contribution due to the interaction between the currents of the projectile and target electron must be added to these theories.

I. INTRODUCTION

In recent years much effort has been devoted to measuring cross sections for K-vacancy production by energetic protons and alpha particles in medium heavy and heavy elements.[1] Most of this work has been done at energies between a hundred keV and 30 MeV per nucleon. Three theories exist that predict the cross sections: the binary-encounter approximation (BEA),[2,3] the plane-wave Born approximation (PWBA),[4] and the semiclassical approximation (SCA).[5] To first order, these theories predict that the K-vacancy cross sections should fit on a universal curve and should be a function only of the K-shell binding energy U_K, the atomic number of the projectile Z_1, and the ratio of the projectile velocity to the velocity of the electron in the K shell, v_1/v_K. Nearly all of the data taken fit the universal curve to within approximately a factor of 2.

K-vacancy production by very relativistic protons has not yet been examined.[1] Nonrelativistically, the cross sections depend on just the ratio v_1/v_K, and hence one can actually examine the high-energy part of the universal curves by measuring K-vacancy production cross sections by moderately energetic protons on very light elements. Thus far, though, these nonrelativistic measurements[6] have not exceeded $v_1/v_K \approx 2.16$. With 4.88-GeV protons, it is possible to obtain $v_1/v_K \approx 5$ (on Ni) which is much larger than any previous measurement. In addition to the large v_1/v_K, however, there is the possibility that additional relativistic effects on the cross sections may be investigated. Previously the highest energy work has been done with 160 MeV protons[7] where no dramatic deviation from the nonrelativistic PWBA theory was found. The cross sections simply decreased roughly as the inverse square of v_1/v_K, as predicted by the PWBA and BEA theories. The authors of that work compared their results with relativistically calculated cross sections for K-vacancy production by incident electrons, suggesting that at proton energies slightly higher than 160 MeV, relativistic effects may cause the cross section to rise again.

We originally undertook this work in order to test whether such a rise in the cross section may be observed at 4.88 GeV. In Sec. II of this paper we present our experimental work and final cross sections, which are higher than the BEA and PWBA theory predictions. To partially explain these deviations we show that an additional term must be added to the BEA or PWBA cross section.

While those theories adequately account for the interaction between the static Coulomb fields of the projectile and target electrons, they neglect the additional interaction between the currents of the two charged particles.[8-11] This current-current interaction should be important in this case since the projectile current has $\beta \approx 1$. In almost all data previously taken, β was small; hence, that contribution could be neglected. The K-vacancy cross sections are calculated in Sec. III and are compared with experimental results in Sec. IV.

II. EXPERIMENT

The experimental configuration is schematically illustrated in Fig. 1. Protons of 4.88 GeV from the Lawrence Berkeley Laboratory Bevatron passed through a 0.0254-mm Ag monitor foil, a 0.00608–0.0508-mm target foil, a scintillation paddle, an ion chamber, and a TV monitor paddle with negligible energy loss. A horizontally placed Si(Li) detector viewed the target at right angles to the beam, and a Ge(Li) planar detector, facing upward, likewise viewed the target at right angles to the beam. The target was tilted vertically by 45° and rotated by 45° so that its normal was 60° to the beam and its plane face was 45° from both the Si(Li) and Ge(Li) detectors. Both detectors also viewed the Ag monitor foil, which was placed 10 cm upstream from the target. To make deadtime corrections, pulses from each detector fired a fast discriminator which supplied one pulse every

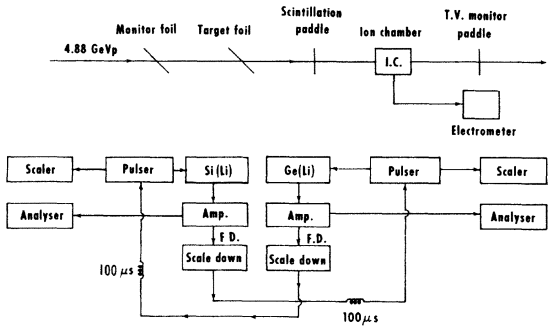

FIG. 1. Schematic diagram showing experimental apparatus layout. FD: fast discriminator; Amp: amplifier, pileup rejector.

hundred pulses to trigger a pulser on the opposite detector. The number of pulses triggered (p_{in}) was recorded, and later the number of pulses counted (p_c) was found. The deadtime correction ($p_{in}/p_c - 1$) varied between 0.4% and 50%.

To monitor the beam intensity, we relied on an ion chamber coupled to an electrometer and integrator to integrate the relative intensity of the beam from run to run. The absolute intensity of the beam was found by irradiating a 0.95-cm-thick graphite target and then we counted off-line the annihilation radiation from the β^+ decay of ^{11}C formed in the reaction $^{12}C(p,pm)^{11}C$. Since the ^{11}C reaction has a known (interpolated) cross section for 4.88-GeV protons, 28 ± 0.6 mb,[12,13] the absolute number of protons passing through the carbon target and ion chamber could be found. Seven calibration runs were taken. The measured number of particles per ion chamber reading varied by less than 2%.

To obtain cross sections insensitive to the uncertainty in the detector deadtime, we measured all of the x-ray yields relative to the yield of Ag $K\alpha$ x rays observed in the monitor foil which, together with the detectors, remained in a fixed position throughout the entire experiment. For some 40 runs we averaged the quantity

$$x = \frac{C(\mathrm{Ag}\,K\alpha)}{R_{IC}} \frac{p_{in}}{p_c}, \qquad (1)$$

where $C(\mathrm{Ag}\,K\alpha)$ is the counts observed in the monitor foil, R_{IC} is the ion-chamber reading, and p_{in}/p_c is the pulser-measured deadtime correction. The yield for an x ray of energy E_x was found by

$$Y = \frac{C(E_x)}{C(\mathrm{Ag}\,K\alpha)} \frac{\langle x\rangle A}{F(E_x)P} \text{ photons/proton}, \qquad (2)$$

where P is the number of protons per ion-chamber reading, $F(E_x)$ is the detector efficiency, $C(E_x)$ is the number of counts observed in the x-ray peak of energy E_x, and A is the correction for air and Be attenuator absorption.

To obtain cross sections, this yield was divided by the target atom density and effective thickness $(1-e^{-\mu t})/\mu$, where t is the thickness of the tilted target and $\mu(E_x)$ is the attenuation coefficient of the target fluorescent x rays in the target material.[14] The cross sections for the $K\alpha$ and $K\beta$ peaks (where separable) were then added, and the neutral-atom fluorescent yield[15] was used to convert the x-ray cross sections to vacancy cross sections.

The uncertainties in these procedures were as follows: (1) Protons per ion chamber reading (counting statistics, ^{11}C cross section, β^+ counter efficiency, graphite target thickness): ±4%; (2) detector efficiency: ±8% Si(Li), ±14% Ge(Li); (3) average number of deadtime corrected Ag $K\alpha$ counts per ion chamber reading ($\langle x\rangle$): ±13% Ge(Li), ±7% Si(Li); (4) target angle, thickness, absorption coefficient: ±2%; (5) counting statistics, including variation from run to run: ±2–10%.

In addition, one other correction for target thickness needs to be made. Plots of the cross sections as a function of target thickness (Fig. 2) show that there is a definite trend for the ob-

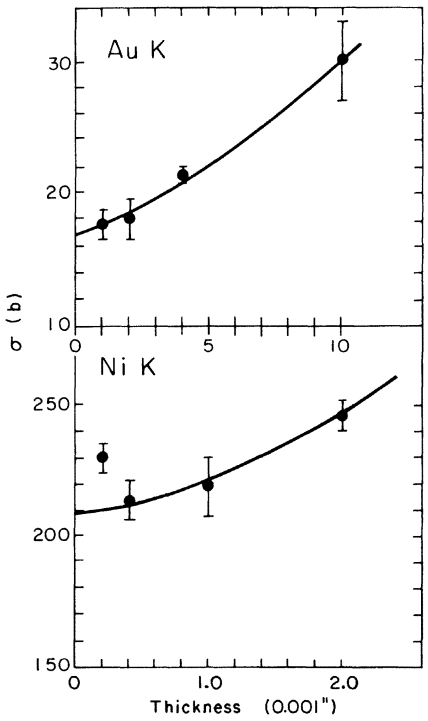

FIG. 2. Experimental cross section versus target thickness. Error bars are relative error only. Curve gives approximation to quadratic thickness dependence.

served cross sections to increase with target thickness. This is due mainly to two secondary processes[7]; (1) protons making energetic secondary electrons in the target which excite K vacancies, and (2) protons making secondary electrons which emit bremsstrahlung radiation in collisions with other target nuclei, which photoelectrically excites K vacancies. For thin targets the former process increases the cross section linearly with target thickness; the latter process increases it quadratically.

To adjust our measured cross sections to zero target thickness, we have used theoretical, though approximate, expressions for processes (1) and (2) and have semiempirically fit these expressions to the data obtained when many different target thicknesses were used. The uncertainty in this correction is at least as large as the correction itself, which in no case was more than 12%. The final cross sections are listed in Table I together with the correction for finite target thickness and the total uncertainty.

III. THEORY

Plane wave Born approximation

The electromagnetic interaction between a swift charged particle and an atomic electron can be subdivided into two terms[8-11]: the unretarded static Coulomb interaction and the interaction between the currents of the two particles. Both are responsible for the transfer of momentum from the projectile to the electron, causing K-vacancy formation. The Coulomb interaction, $Z_1e^2/|\vec{r}-\vec{r}_j|$, where $\vec{r}$ and $\vec{r}_j$ are the position vectors of the projectile and electron, respectively, can be written as a Fourier integral

$$\frac{Z_1e^2}{2\pi^2}\int d\vec{k}\,k^{-2}\exp[i\vec{k}\cdot(\vec{r}-\vec{r}_j)],$$

where $\vec{k}$ serves to transfer momentum from the projectile to the electron.

The current-current interaction may be viewed as the emission and reabsorption of a photon with momentum $\hbar\vec{k}$. Emission of a photon by the incident particle has a matrix element $Z_1ec\vec{\alpha}\cdot\hat{A}_se^{i\vec{k}\cdot\vec{r}}$, where $\hat{A}_s$ is the photon's polarization vector and $\vec{\alpha}$ is the current operator for the particle. Absorption by the electron is proportional to the matrix element of $ec\vec{\alpha}_j\cdot\vec{A}_se^{i\vec{k}\cdot\vec{r}_j}$ where $\vec{\alpha}_j$ is the Dirac matrix for the electron.

Using the PWBA, the cross section for exciting an electron from state 0 to n while simultaneously producing a momentum loss in the projectile of $\vec{q}=\vec{p}-\vec{p}'$ is given by[11]

$$d\sigma_n=\frac{m}{2\pi\hbar^4v_1^2}\,|\langle\vec{p}'n|H_{\rm int}|\vec{p}0\rangle|^2q\,dq, \tag{3}$$

where v_1 is the projectile velocity. From the preceding arguments the matrix element is given by

$$\langle\vec{p}'n|H_{\rm int}|\vec{p}0\rangle=\frac{Z_1e^2}{2\pi^2}\int d\vec{k}\left(k^{-2}\langle\vec{p}'|e^{i\vec{k}\cdot\vec{r}}|\vec{p}\rangle\langle n|\sum_j e^{i\vec{k}\cdot\vec{r}_j}|0\rangle + \sum_s\langle\vec{p}'|\vec{\alpha}\cdot\hat{A}_s\frac{e^{i\vec{k}\cdot\vec{r}}}{k^2-(E_n/\hbar c)^2}|\vec{p}\rangle\langle n|\sum_j\vec{\alpha}_j\cdot\hat{A}_se^{i\vec{k}\cdot\vec{r}_j}|0\rangle\right), \tag{4}$$

where Z_1 is the projectile charge, and E_n ($\equiv E_n-E_0$) is the energy of the excited state. The sum over intermediate states $\sum_s$ includes states where the photon is either emitted first or absorbed first.

The matrix elements depend on the spin of the particle and other relativistic variables, and the square of the matrix element must be averaged over these quantities. For the moment we will neglect these complications, however, and the matrix elements may be reduced, using

$$\begin{aligned}\langle\vec{p}'|e^{i\vec{k}\cdot\vec{r}}|\vec{p}\rangle&=(2\pi)^3\delta(\vec{k}+(\vec{p}'-\vec{p})/\hbar),\\ \langle\vec{p}'|\vec{\alpha}\cdot\hat{A}_se^{i\vec{k}\cdot\vec{r}}|\vec{p}\rangle&=\vec{\beta}\cdot\hat{A}_s(2\pi)^3\delta(\vec{k}+(\vec{p}'-\vec{p})/\hbar),\end{aligned} \tag{5}$$

where $\vec{\beta}=\vec{v}_1/c$.

The first term in Eq. (4) is the Coulomb interaction, which exerts a force parallel to $\vec{q}=\vec{p}-\vec{p}'$ and is therefore called "longitudinal." The inter-

TABLE I. K-vacancy cross sections from 4.88-GeV protons.

Z_2	σ (b)	Finite target thickness correction (%)
Ni	210 ± 25	2.2
Zr	102 ± 12	4.0
Mo	94 ± 12	5.6
Ag	58 ± 10	11.8
Tb	31 ± 7	10.7
Ta	22 ± 4	6.7
Pt	18 ± 4	0.7
Au	17 ± 3	2.8
Pb	15 ± 3	2.7
U	11 ± 3	1.9

action through virtual photons is "transverse" because the photon fields are perpendicular to $\vec{q}$. Following Fano[11] and Eq. (5) we find

$$d\sigma_n = \frac{4\pi Z_1^2 e^4}{v_1^2}\left(\frac{|F_n(q)|^2}{q^4} + \frac{|\vec{\beta}_t \cdot \vec{G}_n(q)|^2}{[q^2 - (E_n/c)^2]^2}\right) q\, dq\,, \quad (6)$$

where $\vec{\beta}_t = \vec{\beta} - (\vec{\beta}\cdot\hat{q})\hat{q}$ is the component of $\vec{\beta}$ perpendicular to $\hat{q}$, and

$$F_n(q) = \sum_j \langle n | e^{i\vec{q}\cdot\vec{r}_j} | 0\rangle\,,$$
$$\vec{G}_n(q) = \sum_j \langle n | \vec{\alpha}_j e^{i\vec{q}\cdot\vec{r}_j} | 0\rangle\,. \quad (7)$$

No interference between the longitudinal and transverse excitations is present because atomic states of different parity are excited by the different interactions.

The evaluation of $F_n(q)$ is well understood.[4] The evaluation of $\vec{G}_n(q)$ has been done also. When n is a continuum state, $\vec{G}_n(q)$ can be recognized as the matrix element for the photoelectric absorption of high-energy photons. In the spirit of the evaluation of $F_n(q)$, nonrelativistic one-electron 1s and continuum wave functions are used, and we equate $\vec{\alpha}_j$ with $\vec{v}_j/c = (iE_n/\hbar c)\vec{r}_j$. Fischer[16] has given

$$|\vec{G}_n(q)|^2 = \frac{E_n^2}{(\hbar c)^2}\,\frac{2^8}{3}\,\frac{Z^6 \exp\{2Z/k \arctan[2Zk/(k^2 - Z^2 - q^2)]\}}{[(q^2 + Z^2 + k^2)^2 - 2q^2k^2]^2[1 - \exp(-2\pi Z/k)]}\,, \quad (8)$$

where $\frac{1}{2}k^2 = \epsilon$ is the continuum energy and Z is the target atomic charge (elsewhere Z_2). To obtain the total K-vacancy cross section, we need only integrate q from $q_{\min} = E_n/\hbar v = (U_K + \epsilon)/\hbar v$ to $q_{\max} = |\vec{p}| \approx \infty$ and over the continuum energy ϵ. Introducing the variables $x = q_{\min}^2/q^2$ and $y = k^2/Z^2$, we find the transverse excitation cross section after a few manipulations:

$$\sigma_K^t = 1.6 \times 10^6 \beta^2 (Z_1^2/Z_2^2) g(\eta_K, \beta^2) \quad \text{(barns)}\,, \quad (9)$$

where $g(\eta_K, \beta^2)$ is a universal function given by

$$g(\eta_K, \beta^2) = \int_0^\infty dy\,(1+y)^{-1} \int_0^1 \frac{(1-x)dx}{(1-\beta^2 x)^2}\,\frac{\exp\{2/\sqrt{y}\,\arctan[2\sqrt{y}/(y-1-P)]\}}{[(P+1+y)^2 - 2yP]^2[1 - \exp(-2\pi/\sqrt{y})]}\,, \quad (10)$$

with $P = (1+y)^2/4\eta_K x$ and $\eta_K = (v_1/v_K)^2$.

We shall discuss the numerical evaluation of $g(\eta_K, \beta^2)$ over a wide range of β^2 and η_K in a later publication. Here, we shall concentrate our attention on the case where $\beta^2 \approx 1$ and the integral over x is strongly peaked at $x = 1$. We can approximate Eq. (10) by letting $x = 1$ for all but the peaking factor, reducing the double integral to two single integrals:

$$g(\eta_K, \beta^2) \approx \int_0^1 \frac{(1-x)\,dx}{(1-\beta^2 x)^2} \int_0^\infty \frac{dy\,(1+y)^{-1} \exp\{2/\sqrt{y}\,\arctan[2\sqrt{y}/(y-1-P)]\}}{[(P+1+y)^2 - 2yP]^2[1 - \exp(-2\pi/\sqrt{y})]} = [\ln(\gamma^2) - \beta^2]/\beta^4 g'(\eta_K)\,, \quad (11)$$

where P is now $(1+y)^2/4\eta_K$ and $\gamma = [1-\beta^2]^{-1/2}$. We have found numerically that $g'(\eta_K)$ is a slowly varying function which changes from 5.7×10^{-3} for $\eta_K = 1$ to 6.6×10^{-3} for $\eta_K = \infty$.

Finally, it may be shown that in the limits of $q_{\min} \approx 0$ or $\eta_K \approx \infty$, one may evaluate $G_n(q)$ by making the dipole approximation, i.e., setting $e^{i\vec{q}\cdot\vec{r}} = 1$. The matrix element is then the same as that given by Bethe and Salpeter[17] and, following a similar analysis, we obtain $g'(\eta_K \approx \infty) = 6.6 \times 10^{-3}$. Hence in the dipole approximation, the transverse cross section is given by

$$\sigma_K^t = 1.056 \times 10^4 \frac{Z_1^2}{Z_2^2}\,\frac{\ln(\gamma^2) - \beta^2}{\beta^2} \quad \text{(barns)}\,. \quad (12)$$

For 4.88-GeV protons one can either numerically evaluate Eq. (10) or Eq. (11) or use the dipole approximation, Eq. (12). The difference between Eq. (10) and Eq. (12) is largest for uranium K-vacancy production. There the two evaluations differ by 10%. To compare with experiment (Fig. 3), we numerically integrated Eq. (10). Screening factors[4] have not been introduced into the evaluation of the transverse cross section, however.

The total K-vacancy production cross section is given by adding the longitudinal contribution to the transverse:

$$\sigma_K = \sigma_K^l + \sigma_K^t\,. \quad (13)$$

The longitudinal cross section was obtained using Khandelwal's[18] tables and includes screening factors.

IV. DISCUSSION

Figure 3 shows the ratio of experimental to theoretical K-vacancy production cross sections versus the target atomic number. The experimental cross sections lie a factor of 1.4 to 2.5 higher

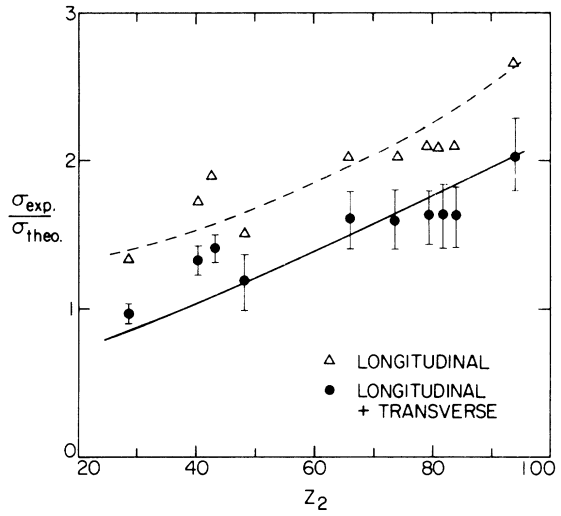

FIG. 3. Ratios of experimental cross sections for 4.88-GeV protons to theory. Lines are drawn to guide the eye only. Error bars are included for $\sigma_{exp}/(\sigma^{l}_{PWBA} + \sigma^{t}_{PWBA})$ only.

than the longitudinal cross sections. The transverse excitation contribution clearly brings the PWBA evaluation closer to experiment, though perfect agreement is still not obtained. It is curious that the deviations are more pronounced for the higher-Z elements where η_K is smallest and indeed overlaps previous measurements. Whether this indicates the importance of a relativistic term in $(\alpha Z)^n$ we cannot say.

It has been pointed out that the Bethe approximation[19,20] agrees quite well with our experimental results. The Bethe approximation incorporates the transverse as well as longitudinal contributions, but is based on the dipole approximation to matrix elements of $e^{i\vec{q}\cdot\vec{r}}$ and $\vec{\alpha}e^{i\vec{q}\cdot\vec{r}}$. The approximation predicts a ratio of experiment to theory of 1.4 for Ni and 1.0 for U which is considerably better than our evaluation. However, the use of the dipole approximation is probably not justified where $qa_K \sim [4\eta_K]^{1/2}$ is of the order of 0.1–0.5 instead of 0. While the dipole approximation to the transverse contribution is justified [see Eq. (11)], it is not for the longitudinal contribution. Comparing Khandelwal's[18] universal function $f(\eta_K, \theta_K \sim 1)$ for the longitudinal cross section with the dipole approximation to it, we find serious disagreements for $\eta_K \lesssim 5$ ($Z_2 \gtrsim 60$ for 4.88-GeV protons). The matrix element of $e^{i\vec{q}\cdot\vec{r}}$ is smaller than the dipole approximation; hence, the better agreement for the high-Z low-η_K elements is fortuitous.

We have used the PWBA to calculate the transverse excitation contribution to systems other than 4.88-GeV protons. Basically, the contribution is negligible in all heavy-particle data that have ever been taken. For instance for 30-MeV p+Ti, the contribution only increases σ_K by a factor of 1.00033. The second highest velocity measurement was made with 160-MeV protons by Jarvis *et al.*[7] There, the factor ranges from 1.0042 for Ti to 1.0026 for U. These results are not surprising, since in all of these cases, the projectile current has $\beta^2 \ll 1$. Hence, the current-current interaction is expected to be small.

Finally we show how the total PWBA cross section behaves at even higher energies. Since the longitudinal cross section depends only on the ratio of the projectile velocity to the K electron velocity, the higher-energy behavior of this cross section is expected to be constant for $E \gtrsim 5$ GeV. However, the transverse contribution rises like the $\log\gamma^2$; hence the total cross section also rises. Figure 4 shows the K cross sections for protons on Sn as a function of kinetic energy up to 10 000 GeV. It is interesting now to return to the point made by Jarvis *et al.*[7] By comparing proton-induced K excitation cross sections with relativistically calculated electron-induced K excitation cross sections, they had previously suggested the kind of rise that is shown in this curve. The reason the electron K excitation curve rises is because of the transverse term. In fact, the behavior of the longitudinal and transverse contributions in the electron theory[21] is qualitatively similar to that displayed in Fig. 4. The longitudinal part approaches a constant to high incident electron energies, while it is the transverse contribution that causes the cross section to rise.

V. CONCLUSIONS

Cross sections for K-vacancy production by 4.88-GeV protons were measured, and they disagreed significantly with the BEA and PWBA predictions.

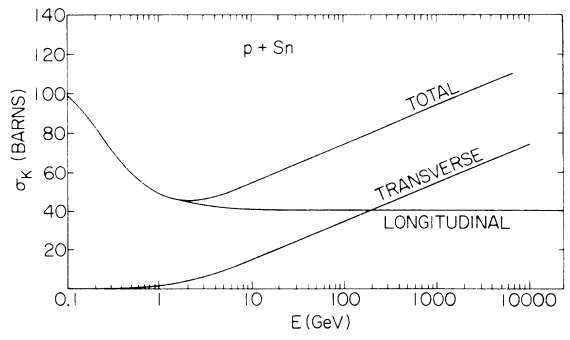

FIG. 4. Very-high-energy behavior of p+Sn cross section calculated by using the PWBA.

We argue that the BEA and PWBA theories of K-vacancy production are correctly extended to relativistic energies when the correct velocity $v_1 = \beta c$ is used in the scaling parameter $(v_1/v_K)^2$. Those theories only account for the interaction between the static Coulomb fields of the projectile and target electrons. Besides this, a contribution due to the interaction between the projectile and electron currents must be added to these cross sections.

The transverse interaction between charged particles and matter has previously been included in calculations of stopping powers[11] and K-vacancy production by incident electrons.[21] The reason why it has not been mentioned in connection with K-vacancy production by protons and heavy ions is because in all previous measurements of this kind the incident projectile velocity had $\beta \ll 1$, and the transverse term was entirely negligible. Many relativistic proton accelerators exist throughout the world, and we hope that this experiment will inspire others to more fully examine the contribution of the transverse interaction to inner-shell vacancy production.

ACKNOWLEDGMENTS

We are indebted to the operating staff of the BEVALAC for their great support. We gratefully acknowledge the encouragement of Professors Sakai, Sugimoto, Nakai, Chamberlain and Steiner. We acknowledge valuable comments on this work from E. Merzbacher, M. Inokuti, Y. K. Kim, J. Wu, J. McGuire, and J. D. Jackson. This report was done with partial support from the United States Energy Research and Development Adminstration.

---

*Present address: Dept. of Physics, Stanford University, Stanford, Calif. 94305.

[1]J. D. Garcia, R. J. Fortner, and T. M. Kavanagh, Rev. Mod. Phys. 45, 111 (1973).
[2]J. D. Garcia, Phys. Rev. A 1, 280 (1970).
[3]J. H. McGuire and P. Richard, Phys. Rev. A 8, 1374 (1973).
[4]E. Merzbacher and H. Lewis, *Encyclopedia of Physics* (Springer-Verlag, Berlin, 1958), Vol. 34, p. 166.
[5]J. Bang and J. M. Hansteen, K. Dan. Vidensk. Selsk. Mat.-Fys. Medd. 31, No. 13 (1959).
[6]Measurements for 18-MeV proton+carbon ($v_1/v_K = 5.9$) were recently reported by D. Burch, Phys. Rev. A 12, 2225 (1975).
[7]O. N. Jarvis, C. Whitehead, and M. Shah, Phys. Rev. A 5, 1198 (1972); and Harwell Report No. AERE-R-6612, 1970 (unpublished).
[8]C. Møller, Ann. Phys. (Leipz.) 14, 531 (1932).
[9]H. Bethe, Z. Phys. 76, 293 (1932).
[10]U. Fano, Phys. Rev. 102, 385 (1956).
[11]U. Fano, Annu. Rev. Nucl. Sci. 13, 1 (1963).
[12]J. B. Cummings, Annu. Rev. Nucl. Sci. 13, 260 (1963).
[13]For more recent values of the ^{11}C cross section we refer to A. Smith, LBL, private communication.
[14]W. H. McMaster, N. Kerr Del Grande, and J. H. Mallett, Report No. UCRL-50174, Sec. II, 1969 (unpublished).
[15]W. Bambynek, B. Craseman, R. W. Fink, H.-U. Freund, H. Mark, C. D. Swift, R. E. Price, and P. Venugopula Rao, Rev. Mod. Phys. 44, 716 (1972).
[16]J. Fischer, Ann. Phys. (Leipz.) 8, 821 (1931).
[17]H. Bethe and E. E. Salpeter, *Encyclopedia of Physics* (Springer-Verlag, Berlin, 1957), Vol. 24, Sec. 71.
[18]G. S. Khandelwal, B. H. Choi, and E. Merzbacher, At. Data 1, 103 (1969). The Ni point in Fig. 3 involves an extrapolation beyond the end of this table and is consequently uncertain.
[19]M. Inokuti, Rev. Mod. Phys. 43, 297 (1971).
[20]Calculations made by Y.-K. Kim, M. Inokuti, E. Merzbacher, and J. Wu, private communications.
[21]H. Kolbentsvedt, J. Appl. Phys. 38, 4785 (1967).